Improved Calculation Method for Insulation-based Fire Resistance of Composite Slabs

Jian Jiang, Adam Pintar, Jonathan M. Weigand, Joseph A. Main, and Fahim Sadek
National Institute of Standards and Technology (NIST), 100 Bureau Drive, Stop 8611, Gaithersburg, MD, USA, 20899

Abstract

Floor slabs play a critical role in the fire resistance of buildings, not only by maintaining structural stability and integrity, but also by providing thermal insulation to limit the rise in temperature of floors above a fire. Composite slabs, consisting of concrete topping on steel decking, are common in steel building construction, but the profiled geometry of the decking makes the analysis of heat transfer in composite slabs more complex than for flat slabs. A method for calculating the insulation-based fire resistance of composite slabs with profiled steel decking is provided in Annex D of Eurocode 4 (EC4). However, the applicability of the EC4 calculation method is limited to a range of commonly used slab geometries from the 1990s, which is narrower than the range used in current practice. In addition, the EC4 calculation method assumes a specific value of moisture content for the concrete, and different values of moisture content can significantly affect the fire resistance, as shown in this study. This paper proposes an improved algebraic expression for estimation of the insulation-based fire resistance of composite slabs that explicitly accounts for moisture content and is applicable to an extended range of slab geometries. The proposed expression is developed based on computed values of fire resistance obtained from a validated finite element modeling approach. A set of 54 composite slab configurations are selected for analysis using a sequential experimental design. The accuracy of the proposed method is verified against numerical results for an additional set of 32 slab configurations and is also validated against experimental data. Comparisons of the proposed calculation method with the results of the verification analyses show deviations of less than 15 min in all cases for the insulation-based fire resistance of the composite slabs.

Keywords: composite slab; fire resistance; insulation criterion; calculation method; EC4; slab geometry; moisture content.

1 Introduction

Composite slabs consist of a concrete topping cast on top of profiled steel decking (ANSI/SDI 2017). Composite slabs are commonly used in the construction of steel-framed buildings because of their efficiency in carrying flexural loads and because the decking acts as stay-in-place formwork. Composite slabs are typically lightly reinforced with anti-crack welded wire mesh. Some composite slabs may also contain individual steel reinforcing bars placed within the ribs. Both normal-weight and structural lightweight concrete are commonly used, although structural lightweight concrete has been gaining popularity over normal-weight concrete due to the cost-saving benefits of reducing the overall weight of the structure.

In addition to their essential load-bearing function, floor slabs play an important role in preventing the spread of fires in buildings. For a building element such as a floor slab to demonstrate fire resistance in a standard fire

test, it must not only maintain structural stability and integrity, but it must also provide thermal insulation, thus limiting the increase in temperature on the cold side of a fire-exposed element (see Phan et al. 2010, Section 2.6). Fire resistance according to the thermal insulation criterion is specified in current standards as the time required for an average temperature rise of 140 °C or a maximum temperature rise of 180 °C, whichever governs, to be reached at the unexposed surface of the slab when the slab is subjected to a standard fire (ASTM 2018, ISO 2014).

The presence of the ribs in composite slabs creates an orthotropic profile, resulting in thermal gradients and structural responses that are more complex than those for flat slabs, presenting challenges in numerical analysis and practical design for fire effects. Jiang el al. (2017a) provided a review of the state-of-the-art in thermal and structural modeling of composite slabs, and some significant contributions relevant to insulation-based fire resistance are summarized in the following. Researchers from the Netherlands Organization for Applied Scientific Research (TNO) developed a thermo-mechanical model of fire-exposed composite slabs, which was validated against a series of fire tests (Hamerlinck et al. 1990; Hamerlinck 1991; Both et al. 1992; Both 1998). Based on the work of Both (1998), an analytical expression to determine the fire resistance of composite slabs was specified in Annex D of Eurocode 4 Part 1.2 (CEN 2005) (hereafter refer to as EC4). The EC4 calculation method and its limitations are presented below in Section 2. Huang et al. (1996) found that the effect of moisture content of concrete should be explicitly considered in the thermal analysis of concrete slabs. Lamont et al. (2001) simulated the thermal responses of composite slabs in the Cardington fire tests, exploring the influence of steel decking, thermal properties of concrete, and slab thickness on the temperature distribution in the slab. The results showed that moisture content had a significant influence on the temperature distribution in composite slabs. Lamont et al. (2004) conducted heat transfer analyses on composite slabs under non-standard fire conditions. The slabs were simulated by 8-node reduced integration shell elements in ABAQUS. The effect of temperature distribution in the composite slabs on the structural behavior was investigated, and the authors emphasized the need for quantitative estimation of fire-induced structural performance for different design fire scenarios. Pantousa and Mistakidis (2013) found that the temperatures obtained from advanced thermal analysis were higher than those determined from the simplified method in EC4, leading to smaller fire resistances than those based on EC4. These differences were most significant in the steel decking. On the other hand, Li et al. (2017) conducted four full-scale fire tests on composite floors, and the values of fire resistance obtained from the experiments were larger than those based on the EC4 calculation.

To overcome the limitations of the existing EC4 calculation method, this study proposes an improved algebraic expression for estimating the fire resistance of composite slabs according to the thermal insulation criterion. The proposed expression was developed based on computed values of fire resistance obtained using a high-fidelity finite element modeling approach, which was validated against experimental results in an earlier study (Jiang et al. 2017a). A sequential experimental design was used to develop a set of 54 composite slab configurations for numerical analysis, and statistical methods were used to identify the factors that most strongly influenced the computed fire resistance, considering main effects and two-way interactions between factors. A new algebraic expression was developed to account for the most significant factors and their interactions, and the coefficients of this expression were determined by minimizing deviations from the set of 54 numerical results. The new expression was then verified against numerical results from a set of 32 additional

composite slab configurations, which were not used in the development of the expression, and validated against experimental results available in the literature.

2 EC4 calculation method for fire resistance of composite slabs

Annex D of EC4 provides a method for estimating the fire resistance of composite slabs according to the thermal insulation criterion based on the work of Both (1998). No revisions have been made to these methods over the past two decades. The fire resistance is determined in Eq. (1) according to the thermal insulation criterion described previously.

$$t_i = a_0 + a_1 \cdot h_1 + a_2 \cdot \Phi_{\text{up}} + a_3 \cdot \frac{A}{L_r} + a_4 \cdot \frac{1}{l_3} + a_5 \cdot \frac{A}{L_r} \cdot \frac{1}{l_3} \tag{1}$$

Figure 1 illustrates a typical temperature distribution in a composite slab exposed to fire, indicating the maximum and average temperature values considered in the thermal insulation criterion. In Eq (1), h_1 is the thickness of the continuous upper portion of the slab (see Figure 1), Φ_{up} is the view factor of the upper flange of the steel decking, A/L_r is the rib geometry factor, defined as the ratio of the concrete volume to the exposed surface area, and l_3 is the width of the upper flange. The values of coefficients $a_0 - a_5$ are specified in EC4 for normal-weight and lightweight concrete.

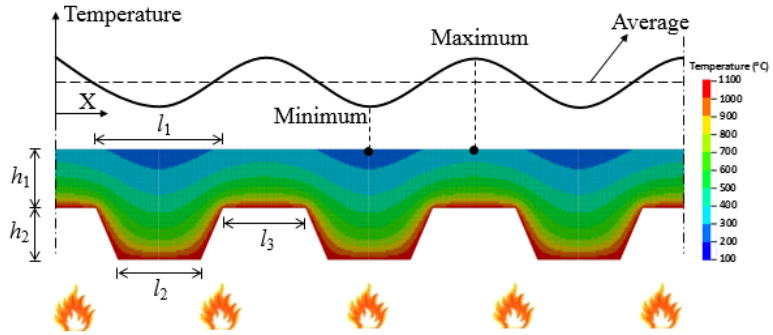

Figure 1. Temperature distribution in a composite slab exposed to fire.

The view factor Φ depends on the area and orientation of the surface emitting radiation relative to the surface receiving radiation, as well as the distance between them. For composite slab geometries, the view factor of the lower flange of steel decking is typically taken as unity, $\Phi_{\text{low}} = 1.0$. The view factors for the web and upper flange of steel decking are less than unity due to obstruction by the ribs. They are calculated in EC4 based on Hottel's crossed-string method (Nag 2008), which accounts for the specific rib geometry, giving the following equations for the upper flange and web of the decking, respectively.

$$\Phi_{\text{up}} = \frac{\sqrt{h_2^2 + \left(l_3 + \frac{l_1 - l_2}{2}\right)^2} - \sqrt{h_2^2 + \left(\frac{l_1 - l_2}{2}\right)^2}}{l_3} \tag{2a}$$

$$\Phi_{\text{web}} = \frac{\sqrt{h_2^2 + \left(\frac{l_1 - l_2}{2}\right)^2} + (l_3 + l_1 - l_2) - \sqrt{h_2^2 + \left(l_3 + \frac{l_1 - l_2}{2}\right)^2}}{2\sqrt{h_2^2 + \left(\frac{l_1 - l_2}{2}\right)^2}} \tag{2b}$$

The EC4 calculation method in Eq. (1) has three significant limitations:

(1) The EC4 calculation method was developed for a specific range of geometric parameters of commonly used steel decking in the 1990s, which is narrower than the range used in current steel construction practice. A survey by the authors on recent experimental and numerical studies of composite slabs, along with a review of manuals from steel decking manufacturers, showed that the range of geometries in common applications of steel decking has expanded beyond the range specified in EC4, as shown in Table 1 (see dimensions in Figure 1). The applicability of the EC4 fire resistance calculation for this extended range of slab geometries requires further examination. A preliminary study by Jiang et al. (2017b) found that the EC4 calculation method provided reasonable estimates of fire resistance for slabs within the range of geometries specified in EC4 but could significantly underestimate or overestimate the fire resistance for geometries beyond the specified range. These effects were more pronounced for deep ribs (large h_2), wide ribs and upper flanges (large l_1 and l_3), and narrow lower flanges (small l_2).

(2) The EC4 calculation method does not consider the effect of various levels of moisture content of concrete on the fire resistance of composite slabs. The EC4 calculation assumes a moisture content of 4 % and 5 % for normal-weight and lightweight concrete, respectively, and thus does not capture the considerable range of moisture content that can be found in real structures (e.g., the practical moisture content of concrete may reach up to 10 % (CEN 2005)). The moisture content has a significant influence on the temperature at the unexposed surface of the slab (Jiang et al. 2017a). Thus, it is important to consider the influence of the moisture content on the fire resistance of composite slabs.

(3) The calculation method in EC4 was formulated based on geometrical parameters that were acknowledged to have been selected "to some extent arbitrarily" (Both 1998). Rather than using a rigorous statistical approach, the process of selecting the parameters used in the calculation method "was based on general considerations with respect to heat transfer to and heat flow in fire-exposed composite slabs" (Both 1998). As can be seen in Eq. (1), only interactions between A/L_r and $1/l_3$ were included, and other interactions were neglected without verification.

Table 1. Comparison between EC4 and practical range for dimensions of composites slabs

Range of slab geometries	h_1 (mm)	h_2 (mm)	l_1 (mm)	l_2 (mm)	l_3 (mm)
EC4	50 to 125	50 to 100	80 to 155	32 to 132	40 to 115
Practice	50 to 125	40 to 100	50 to 240	30 to 160	40 to 150

Deviations resulting from these limitations are illustrated subsequently in Section 3.3, in which fire resistance values from Eq. (1) are compared with numerically computed values obtained using a high-fidelity finite element modeling approach that is described in the following sections.

3 Numerical simulation of heat transfer in composite slabs

3.1 High-fidelity modeling

The high-fidelity finite-element modeling approach used in this study was previously validated by the authors against experimental results available in the open literature (Jiang et al. 2017a). In this approach, the concrete slab was modeled with solid elements and the steel decking was modeled with shell elements. The concrete slab and steel decking had a consistent mesh at their interface and shared common nodes. Noting the periodicity of the composite slab profile and the uniformity of the thermal loading, only one half-strip of the composite slab was modeled, as shown in Figure 2. Adiabatic boundary conditions were assigned at the right and left boundaries of the model to represent the symmetry at these sections in the periodic slab profile. Convection and radiation boundary conditions were defined at the top surface of the slab and at the bottom surface (i.e., the lower flange, web, and upper flange labeled in Figure 2) of the steel decking. In the analyses, the ISO 834 standard fire curve (ISO 2014) was used to determine the gas temperature at the fire-exposed surface of the slabs. The heat transfer analyses were performed using the LS-DYNA finite-element software (LSTC 2014). Both the concrete and the steel decking were modeled using an isotropic thermal material model, with the specific heat and thermal conductivity for each material defined as functions of temperature using the equations specified in EC4. Figures 3 and 4 show, respectively, the temperature-dependent specific heat and thermal conductivity for concrete based on EC4 that are used in this study. Similar to Both (1998), the upper limit for the thermal conductivity of normal-weight concrete was used based on Figure 4.

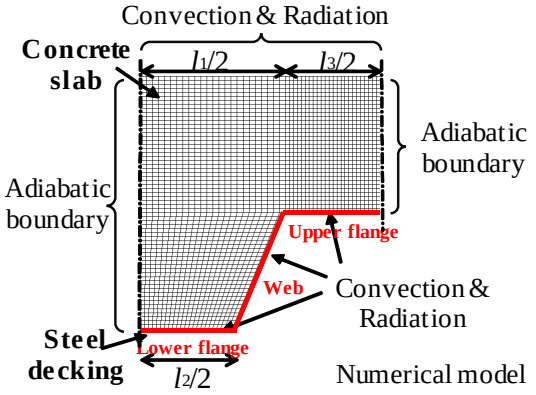

Figure 2. High-fidelity thermal model of composite slab

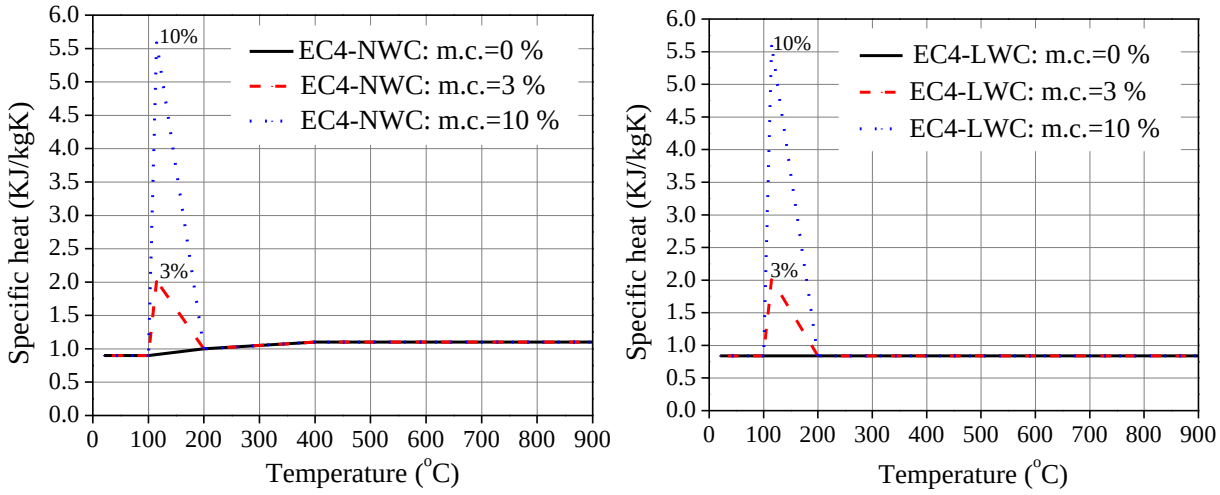

Figure 3. Specific heat of concrete in EC4: (a) normal-weight concrete (NWC); (b) lightweight concrete (LWC)

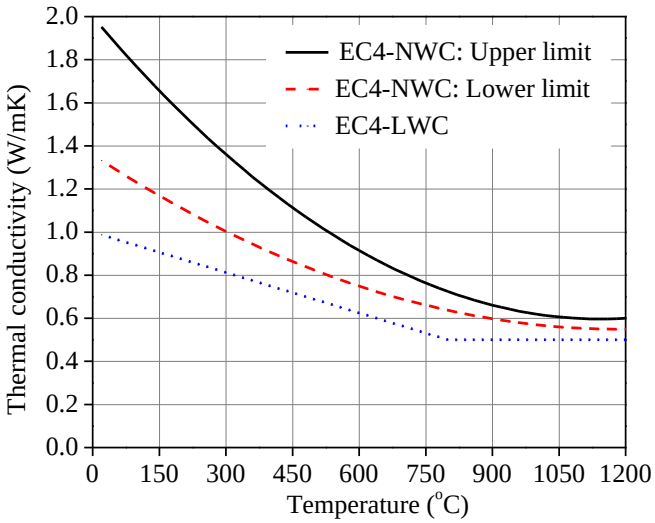

Figure 4. Thermal conductivity of concrete in EC4

Based on previous validation studies (Jiang et al. 2017a), the parameters proposed by Both (1998) for use in the EC4 calculation method were revised (see Table 2) to obtain a better prediction of the temperature distribution. These revisions included the following: (1) using a convective heat transfer coefficient of 4 W/(m^2·K) instead of 8 W/(m^2·K) used in the EC4 method, for the unexposed top surface of the slab. The value of 4 W/(m^2·K) is specified in EN 1991-1-2; (2) using a temperature-dependent emissivity of steel (0.1 for T < 400 °C and 0.7 for T > 800 °C) to account for the effect of the melting of the zinc layer instead of (0.1 for T < 400 °C and 0.4 for T > 800 °C) assumed by Both (1998). The higher emissivity of 0.7 (rather than 0.4) at high temperature was taken as recommended in EC4, leading to better agreement with experimental results at high temperatures (Jiang et al. 2017a); and (3) using a range of 3 % to 10 % for the moisture content of the concrete slab, compared to a constant value of 4 % for normal-weight concrete and 5 % for lightweight concrete in the EC4 method. The revised convective heat transfer coefficient and emissivity of steel had a smaller contribution to the differences between the results by Both (1998) and those reported herein, compared to the

contribution of the range of moisture content considered in this study. As noted earlier and shown in Table 1, the analyses in this study considered a wider range of decking geometries than did Both (1998).

Table 2. Comparison of parameters used in the EC4 and proposed calculation method

Parameter	**EC4 method (Both 1998)**	**Proposed method**
Thermal Boundary Conditions		
Gas temperature	ISO 834	ISO 834
Convective heat transfer coefficient for fire-exposed decking, $h_{c,deck}$	Lower flange: 25 W/(m^2·K) Web, upper flange: 15 W/(m^2·K)	Lower flange: 25 W/(m^2·K) Web, upper flange: 15 W/(m^2·K)
Convective heat transfer coefficient for unexposed top surface, $h_{c,top}$	8 W/(m^2·K)	4 W/(m^2·K)
Emissivity of decking, $\varepsilon_{s,deck}$	T < 400 °C: 0.1 T > 800 °C: 0.4	T < 400 °C: 0.1 T > 800 °C: 0.7
Emissivity of concrete, $\varepsilon_{s,top}$	0.78	0.7
Properties of Concrete		
Moisture content, m.c.	NWC: 4 % LWC: 5 %	NWC: 3 % to 10 % LWC: 3 % to 10 %
Density	NWC: 2350 kg/m^3 LWC: -	NWC: 2300 kg/m^3 LWC: 1900 kg/m^3

Note: NWC denotes normal-weight concrete and LWC denotes lightweight concrete.

3.2 Typical temperature distribution in composite slabs

Figure 1 shows a typical temperature distribution in a composite slab with standard fire exposure from below, and Figure 5 shows corresponding temperature histories at various locations through the depth of the composite slab. The temperature contours in the slab (Figure 1) exhibit curved isotherms that generally follow the profile of the steel decking, with reduced curvature of the isotherms near the top surface of the slab. During fire exposure, heat is input from the fire to the bottom of the slab by means of convection and radiation. Fireproofing is not typically applied to the steel decking, and therefore the temperature of the decking rises rapidly (Points A and F in Figure 5). The web and upper flange of the decking have slightly lower temperatures than the lower flange due to the shielding effect of the rib (e.g., compare the temperature histories for points A and F in Figure 5). Because of the large heat capacity of the concrete, the temperature of the steel decking is significantly lower than the gas temperature in the early stages of heating but approaches the gas temperature in the later stages (compare temperature histories for points A and F with the gas temperature in Figure 5). As shown in Figure 5, the temperature increase within the concrete slab is slower than that of the steel decking, with higher temperatures occurring in the thin portion of the slab (Points F, G, and H) than in the thick portion (Points A, B, D, and E). This results in a non-uniform temperature distribution at any height through the thickness of the upper continuous portion of the slab. Thus, the temperature of the reinforcement mesh in the thin portion (e.g., at Point G) will be higher than that in the thick portion (e.g., Point D). The maximum temperature at the

unexposed surface of the slab occurs at Point H, and this temperature typically controls the thermal insulation provided by the composite slab.

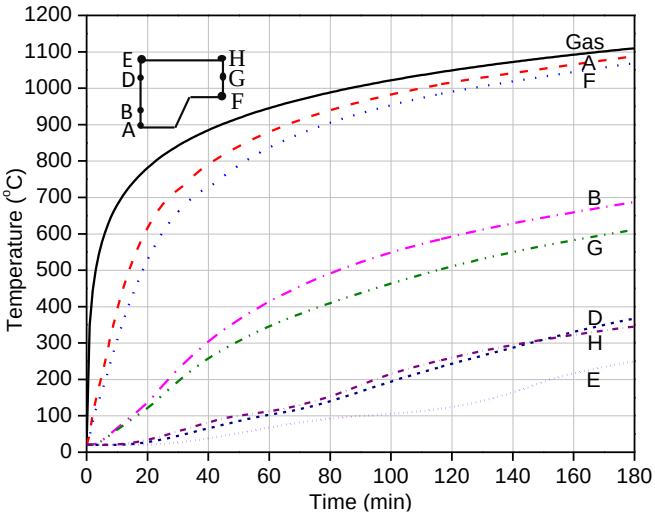

Figure 5. Typical temperature histories at selected locations in a composite slab

The parametric study by Jiang et al. (2017b) showed that moisture content had a significant influence on temperatures in the slab, especially at the unexposed surface. During heating, evaporation of moisture occurs, absorbing energy and thus delaying the temperature rise in the concrete. The effect of evaporation of free moisture in concrete is commonly modeled by modifying the specific heat within a certain temperature range. Migration of moisture also occurs but is typically ignored. Free moisture is assumed to evaporate within a temperature range of 100 °C to 200 °C. For instance, a peak specific heat at 115 °C is assumed in EC4 for both normal-weight and lightweight concrete. This approach in the heat transfer analysis is normally appropriate in fire engineering calculations. The results by Jiang et al. (2017b) showed a reduction in the rate of temperature increase as the temperature passed 100 °C. This effect was more significant for higher values of moisture content, leading to longer delays in the temperature rise within the concrete, and a plateau in the temperature history becomes evident for the moisture content of 7 % or higher. After most of the moisture has evaporated (at temperatures exceeding about 150 °C), the temperature in the concrete rises more rapidly.

3.3 Comparison of fire resistances between EC4 and numerical results

Figure 6 presents a comparison of fire resistance values obtained from the EC4 calculation method (Eq. 1) with numerical results obtained using the finite element modeling approach described in Section 3.1. The results in Figure 6 correspond to a set of 54 different composite slab configurations, which were developed using a sequential experimental design, as described in the following section. The results in Figure 6 are also presented in Table A.1 in the Appendix, along with the slab dimensions, moisture content, and concrete type for each slab configuration. The results in Figure 6 and Table A.1 show that the EC4 method can overestimate the fire resistance by as much as 26 min (up to 35 %), which is not conservative, and can underestimate the fire

resistance by as much as 154 min (up to 46 %), which is conservative. By using different symbol types for different values of moisture content, Figure 6 clearly shows that the moisture content has a significant effect on the accuracy of the EC4 calculation method, with the largest discrepancies for the largest value of moisture content (m.c. = 10 %). These results further highlight the necessity of an improved calculation method to accurately estimate the fire resistance for an extensive range of slab geometries and moisture content.

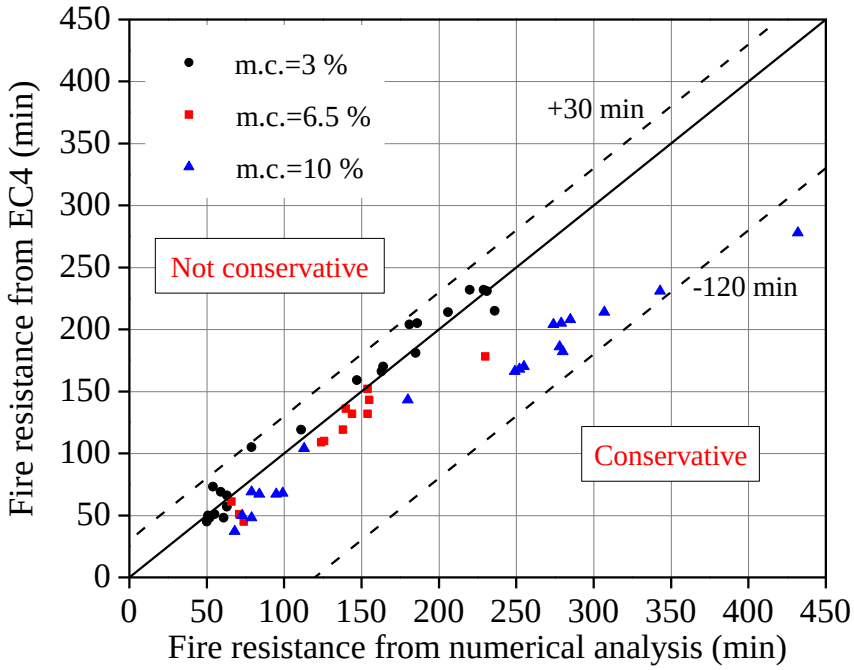

Figure 6. Comparison of EC4 calculations with numerical results for fire resistance of 54 composite slabs in Table A.1

4 New algebraic expression for the fire resistance of composite slabs

A major focus of this work is the development of an improved algebraic expression for the fire resistance of composite slabs. The expression was developed by using the high-fidelity numerical model for targeted combinations of slab geometry, moisture content, and concrete type, and then fitting a low-order polynomial to those observations of fire resistance. Five geometrical variables were considered, in addition to moisture content and concrete type (normal-weight or lightweight). The geometrical parameters included h_1, h_2, l_2, and l_3, along with the parameter $l_{12} = (l_1 - l_2)/2$, which was used as independent parameter instead of l_1 to ensure that l_2 remained less than l_1 (see Figure 1). The development proceeded in two stages. In the first stage, a fractional factorial screening design was employed to identify factors having the largest influence on fire resistance. In the second stage, the screening experiment was augmented to the extent required to fit a full quadratic response surface for each concrete type (normal-weight and lightweight). Separate response surfaces for each concrete type were necessary because concrete type was deemed an important factor in the first stage. A set of 54 composite slabs (Table A.1 in the Appendix) were used to develop the expression, which was verified against another 32 combinations (Table A.2 in the Appendix) of slab geometry, moisture content, and concrete type.

4.1 Screening design

The first 32 slab configurations in Table A.1 comprise the screening design, a resolution IV, 2-level, fractional factorial design in seven factors (five geometrical parameters, moisture content, and concrete type). Examples of representative geometries used in the heat transfer analysis are shown in Figure 7. Note that certain combinations of geometrical parameters might produce steel decking geometries that are not used in practice. Such geometries were used to maintain orthogonality of the screening design and to ensure that all realistic geometries were contained within the convex hull formed by the tested geometries. Heat transfer analyses were conducted using these 32 slabs, assuming up to four hours of fire exposure to the ISO 834 standard fire curve. The main influencing factors were identified by main effects and interactions plots, which follow.

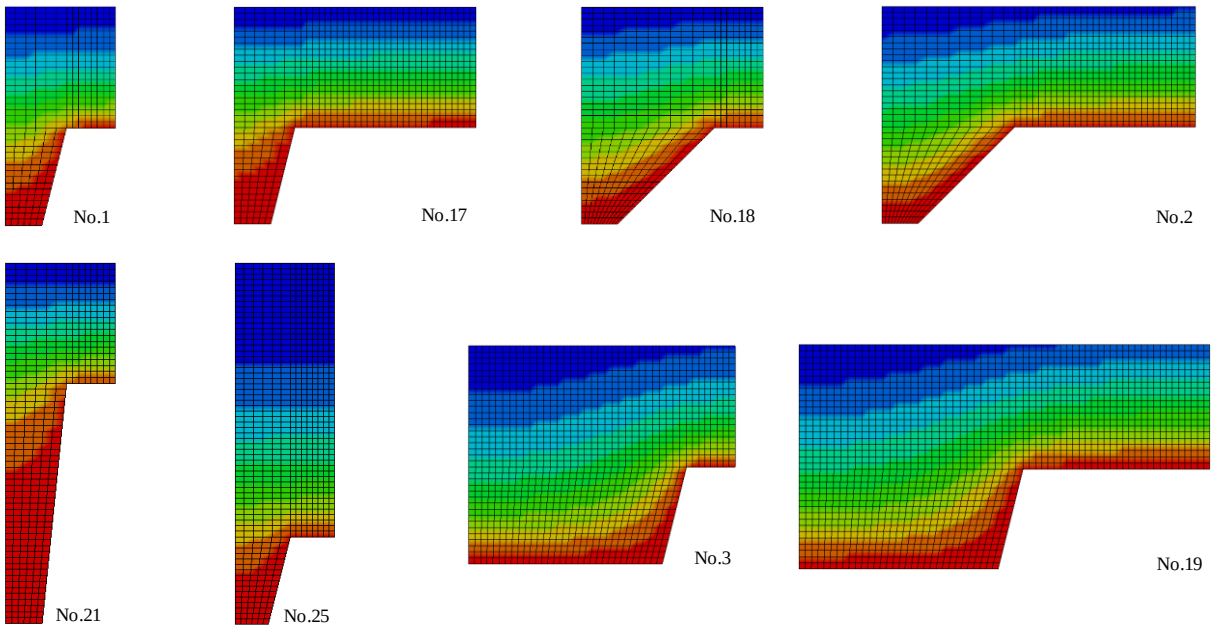

Figure 7. Typical geometries used in the 32 composite slab configurations
Numbers based on Table A.1

4.1.1 Main effects

The main effects plot in Figure 8 identifies the factors having the largest average effect on fire resistance. Clearly, h_1 has the largest main effect, about 87 min, which is half the span between the average fire resistance corresponding to the high and low values of h_1. This should come as no surprise as h_1 has a large impact on the thermal mass of the slab, and consequently the temperatures at the unexposed surface of the slab. Moisture content has the second largest main effect, reinforcing the important influence of moisture content on the fire resistance of the slabs (see Jiang et al. 2017a). The parameter $l_{12} = (l_1 - l_2)/2$ has the smallest average effect on the fire resistance.

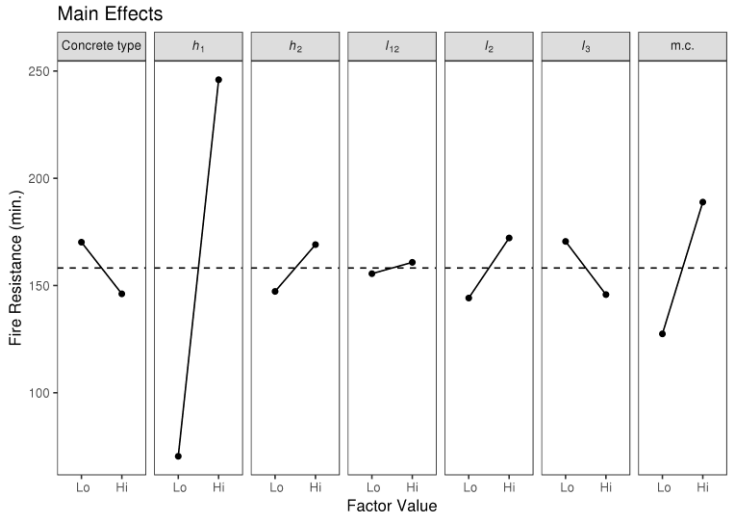

Figure 8. Main effects of influencing factors for fire resistance of composite slabs

4.1.2 Interaction between factors

In addition to the main effects, the screening design also permits the estimation of two-way interactions. Figure 9 shows the values (i.e., numbers specified in min) and relative magnitudes of the 21 two-way interactions (relative to the largest two-way interaction between h_1 and m.c.). Large darkly-shaded circles represent large two-way interactions in relative magnitude, while small lightly-shaded circles represent small ones. As expected, the interaction between h_1 and moisture content is the largest in magnitude, as indicated by having the largest, darkest circle. The two-way interaction between h_1 and moisture content is about 18.5 min. The main effect of h_1 (half of the average difference between high and low) is about 87 min, and combining those two numbers gives the following interpretation: When moisture content is low, the main effect of h_1 is about 87 – 18.5 = 68.5 min, and when moisture content is high, the main effect of h_1 is about 87 + 18.5 = 105.5 min. The three largest two-way interactions all involved h_1. The smallest two-way interaction corresponded to h_2 and concrete type (i.e., normal-weight or lightweight concrete), but note that none of the interactions associated with l_{12} are large relative to the largest two-way interaction. Since l_{12} had the smallest main effect, and all interactions associated with l_{12} were small relative to the largest two-way interaction, l_{12} was dropped from further study, but the rest of the factors were retained.

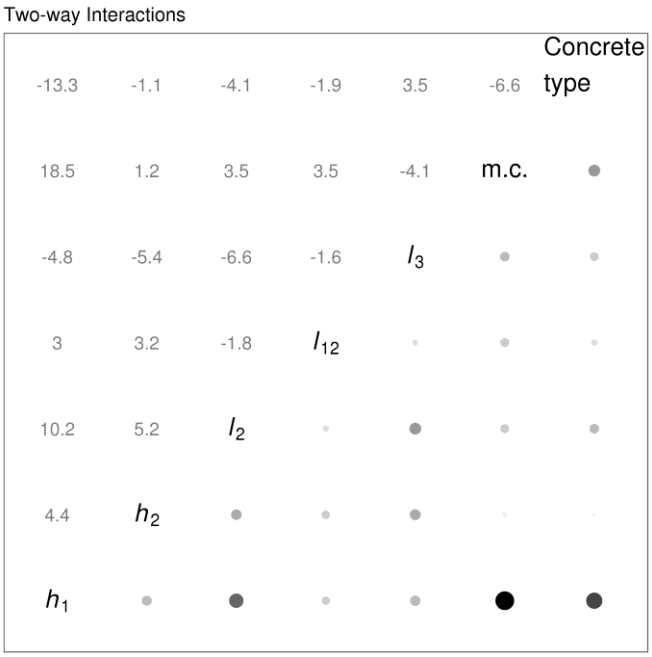

Figure 9. Two-way interactions of influencing factors for fire resistance of composite slabs (numbers specified in min)

4.2 Proposed expression

As a first step, fire resistance results from the 32 slab configurations of the screening design were used to fit a hyperplane intended to serve as the new expression. The hyperplane included all main effects except for l_{12} (since it was deemed insignificant, see Figure 8), as well as the three largest two-way interactions. To check the utility of the fitted hyperplane, 12 runs for slabs with lightweight concrete only, from a previous work, not used to fit the hyperplane, were compared to predictions from the fitted hyperplane. That comparison highlighted the need for a curved surface instead of a planar surface.

The original 32 slab configurations from the screening design were then *D*-optimally augmented using the Federov exchange algorithm (Fedorov 1972) with 20 new configurations (10 each for normal-weight and lightweight concrete) to permit a full quadratic surface to be fitted in 5 factors (the geometry factors excluding l_{12}, in addition to moisture content) separately for normal-weight and lightweight concrete. Two center points were also included to bring the total to 32 + 20 + 2 = 54 runs. A full quadratic surface in five variables has 20 terms: 5 linear terms, 5 pure quadratic terms, and 10 cross terms. The Bayesian Information Criterion (Schwarz 1978) was used to select the best subset of these 20 possible terms in order to provide the simplest possible expression that still provides a good representation of fire resistance from the numerical model. For normal-weight concrete, a model with 11 of the 20 possible terms was selected, and for lightweight concrete, a model with 16 terms was selected.

The expression to estimate the fire resistance of composite slabs is presented in Eq. (3) with associated coefficients for normal-weight and lightweight concrete listed in Table 3. While Eq. (3) looks unwieldy, it is

relatively simple to implement in a spreadsheet or simple computer script. Note that only one of the pure quadratic terms, (h_1^2), was deemed important for both normal-weight and lightweight concrete.

$$t_i = b_0 + b_1 h_1 + b_2 h_2 + b_3 l_2 + b_4 l_3 + b_5[m.c.] + b_6 h_1^2 + b_7 h_1 h_2 + b_8 h_1 l_2 + b_9 h_1 l_3 + b_{10} h_1 [m.c.] + b_{11} h_2 l_2 + b_{12} h_2 l_3 + b_{13} h_2 [m.c.] + b_{14} l_2 l_3 + b_{15} l_2 [m.c.] + b_{16} l_3 [m.c.] \quad (3)$$

Table 3. Coefficients used in Eq. (3) for estimating the fire resistance of composite slabs

	Coefficient value for each concrete type	
Coefficient	Normal-weight concrete	Lightweight concrete
b_0	38.6 min	68.7 min
b_1	−0.2 min/mm	−1.44 min/mm
b_2	−0.057 min/mm	−0.11 min/mm
b_3	−0.13 min/mm	−0.5 min/mm
b_4	−0.082 min/mm	0.79 min/mm
b_5	−118.1 min	−784.2 min
b_6	0.0063 min/mm^2	0.0137 min/mm^2
b_7	0.0023 min/mm^2	0.0056 min/mm^2
b_8	0.0029 min/mm^2	0.0057 min/mm^2
b_9	0	−0.0037 min/mm^2
b_{10}	10.36 min/mm	17.5 min/mm
b_{11}	0.0018 min/mm^2	0.0032 min/mm^2
b_{12}	0	−0.0053 min/mm^2
b_{13}	0	3.6 min/mm
b_{14}	−0.001 min/mm^2	−0.0015 min/mm^2
b_{15}	0	1.67 min/mm
b_{16}	0	−2.6 min/mm

Figure 10 presents a comparison of fire resistance values obtained from Eq. (3) with values obtained from numerical analysis for the 54 slab configurations listed in Table A.1 of the Appendix. The values obtained from Eq. (3) were within 12 min of the numerically computed fire resistance in all cases, with a maximum deviation of 15 %.

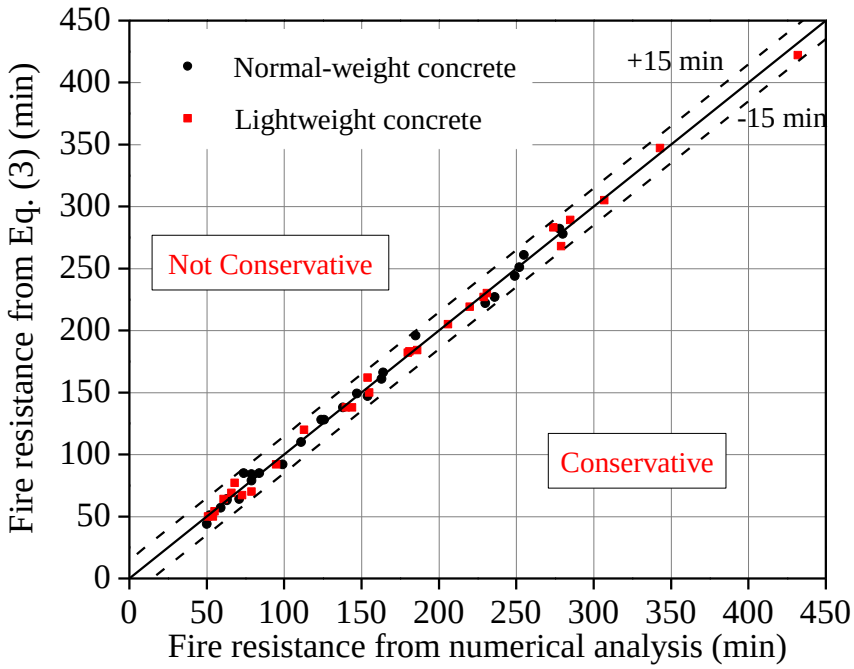

Figure 10. Comparison of proposed expression (Eq. (3)) with numerical results for fire resistance of 54 composite slabs in Table A.1: (a) normal-weight concrete; (b) lightweight concrete

4.3 Verification and validation

The accuracy of the proposed expression (Eq. (3)) was verified using an additional 32 slab configurations (Table A.2 in the Appendix). The 12 lightweight slabs previously mentioned in Section 4.2 were augmented with 20 more slab configurations, 10 with lightweight concrete and 10 with normal-weight concrete. The 20 new slabs were selected using a space filling Latin hypercube design generated by the MaxPro package for the statistical software R (Shan and Roshan 2015; R Core Team 2018). The analysis results are shown in Figure 11 and Table A.2 in the Appendix. The absolute deviations between the proposed expression and the numerical predictions were less than 15 min in all cases (Figure 11), and the percentage deviations were less than 10 % in all cases and less than 5 % in most cases (Table A.2).

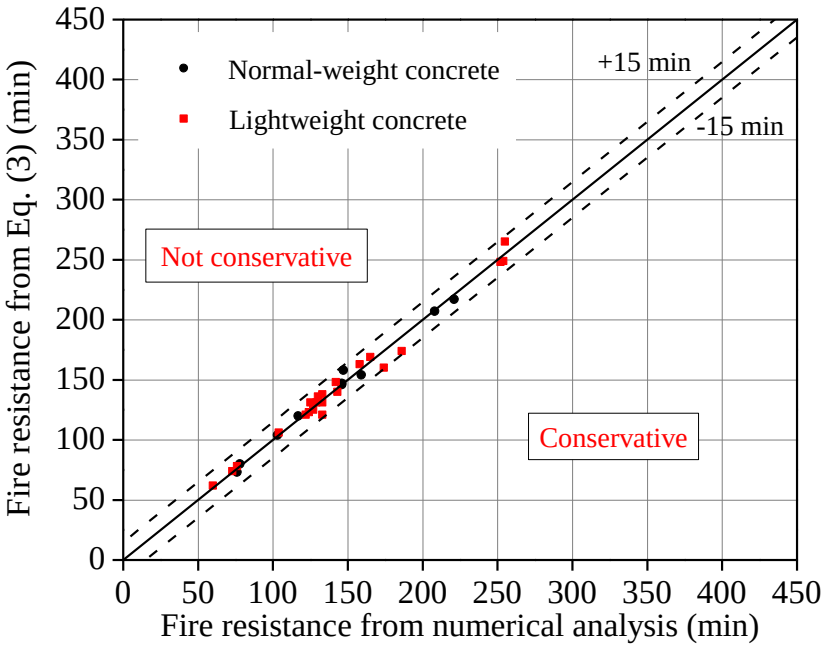

Figure 11. Comparison of proposed expression (Eq. (3)) with numerical results for fire resistance of 32 composite slabs in Table A.2

Table 4 presents experimental results for the insulation-based fire resistance of composite slabs from the literature that are available for validating Eq. (3). While other experimental results for composite slabs in fire are reported in the literature, they are not included in Table 4 because either (a) data on the temperature at the unexposed surface of the slab were not recorded in the tests or (b) the experiments used non-standard fires. For the first three experiments listed in Table 4, the deviation between Eq. (3) and the measured fire resistance was 9 min, and for the fourth experiment, the deviation was 18 min. Because the moisture content was not available for the last two experiments (Zhao et al. 2011 and Bednar et al. 2013), values of fire resistance were estimated from Eq. (3) for two different values of moisture content: 4 % and 10 %. The estimated fire resistance for the higher moisture content of 10 % agreed well with the experimental results. The results in Table 4 show that values of fire resistance based on the proposed expression (Eq. (3)) tended to be close to the experimental results and were conservative in the majority of cases. However, the experimental data were only for normal-weight concrete, and a further validation against lightweight concrete is needed.

Table 4. Validation of the proposed expression against experimental data

Reference	Type of Decking	Slab Dimensions (mm)					m.c.[a] (%)	Concrete type	Fire resistance (min)		Deviation of Eq. (3) from Test (min)
		h_1	h_2	l_1	l_2	l_3			Test	Eq. (3)	
TNO Tests (Hamerlinck 1991)	Prins PSV 73	50	73	84	47	20	3.4	NWC[b]	75	66	−9
	Prins PSV 73	70	73	84	47	20	3.4	NWC[b]	99	91	−8
	PMF CF 60	70	60	169	120	131	4.8	NWC[b]	95	86	−9
	Cofrastra 70	75	70	113	87	70	4.8	NWC[b]	87	105	18
COSSFIRE (Zhao et al. 2011)	COFRAPLUS 60	97	58	101	62	107	-	NWC[b]	180	124[c] 177[d]	−56[c] −3[d]
Bednar et al. (2013)	TR40/160	40	38	110	50	50	-	NWC[b]	75	50[c] 68[d]	−25[c] −7[d]

Notes: a) m.c. = moisture content; b) NWC = normal-weight concrete; c) m.c. = 4 % assumed; d) m.c. = 10 % assumed.

5 Discussion on the influence of moisture content

The results in this study showed that moisture content (m.c.) of concrete has a significant effect on the fire resistance of composite slabs. As Eq. (3) and the associated coefficients in Table 3 indicate, the larger the moisture content, the greater is the fire resistance. Such an effect is not considered by the EC4 calculation, and this could result in a large underestimation of the fire resistance for large values of moisture content, say 10 %. Note that in practice, however, it is generally not possible to determine the actual value of the moisture content of concrete *a priori*, and even if that were possible, the moisture content could change during the service life of the structure. Nevertheless, this study highlights the significance of the effect of moisture content on fire resistance. Further work on evaluation of in situ moisture content in floor slabs would be valuable to provide statistics (e.g., its probability distribution) that could inform a reliability-based approach to consider the variability of moisture content and its influence on fire resistance. Engineers strive for design equations that are both conservative and risk-consistent. If better information on moisture content is available, Eq. (3) would allow engineers to calculate the fire resistance using an appropriate level of conservatism (e.g., expected value of moisture content minus one standard deviation).

It should be noted that in the absence of data on the actual value of the moisture content, it is likely that the engineer uses values based on those assumed by EC4 (4 % and 5 % for normal-weight and lightweight concrete, respectively). Even if these values are used in design, the fire resistance estimated by the proposed expression in this study would be more accurate than that based on the EC4 calculation. To demonstrate this, lightweight concrete with a moisture content of 5 % was used for the ten slabs at the end of Table A.2 (No. 77 to 86), consistent with the moisture content assumed for lightweight concrete in the EC4 method. As the table shows, the differences of fire resistance between the proposed expression and the numerical prediction ranged from −2 % to +4 %, while the differences of fire resistance between the EC4 calculation and the numerical prediction ranged from −11 % to +14 % (positive values indicate overestimation of the fire resistance when compared with the numerically computed value, which is not conservative).

6 Limitations

The proposed expression accurately predicts the fire resistance of composite slabs within ±15 min. Eq. (3) is only applicable to composite steel-concrete composite decks of dimensions bounded by Table 1, and using normal-weight or structural lightweight concrete with moisture contents between 3 % and 10 %. Consistent with the EC4 calculation method, the thermal insulation criterion, not structural failure of the composite slab, was used to evaluate the fire resistance of the composite slab geometries. Obviously, a more sophisticated performance-based design approach would be required to determine the actual structural fire resistance of composite slabs. Such high-fidelity finite-element thermal-structural analysis of composite slabs has been considered by authors in other publications.

7 Summary and Conclusions

This study developed an improved algebraic expression for estimating the fire resistance of composite slabs based on the thermal insulation criterion. The applicability of the EC4 calculation method for an extended range of slab geometries and moisture content of concrete was also examined. The results showed that the EC4 calculation method provided unconservative (up to 35 %) and overconservative (up to 46 %) predictions of fire resistance of composite slabs. The proposed expression for calculation of fire resistance (Eq. (3)) was derived based on an extended range of decking geometries which was more encompassing of geometries used in modern steel construction. In addition, the effect of moisture content (in the range of 3 % to 10 %) was explicitly accounted for. A rigorous statistical approach was implemented to derive the improved expression. The approach included two stages. In the first stage, a fractional factorial screening design was employed to identify factors having the largest influence on fire resistance, while in the second stage, the screening experiment was augmented to fit a full quadratic response surface for each concrete type (normal-weight and lightweight). A set of 54 composite slabs was used to develop the expression, which was verified against another 32 combinations of slab geometry, moisture content, and concrete type. Comparisons of the proposed calculation method with the results of the verification analyses showed deviations of less than 15 min in all cases for the insulation-based fire resistance of the composite slabs. The proposed expression was also validated against a limited set of available experimental data, and the largest deviation from the experimental results was 18 min.

Disclaimer

Certain commercial entities, equipment, products, or materials are identified in this document in order to describe a procedure or concept adequately. Such identification is not intended to imply recommendation, endorsement, or implication that the entities, products, materials, or equipment are necessarily the best available for the purpose.

References

1. American National Standards Institute/Steel Deck Institute (ANSI/SDI). (2017). C-2017 Standard for Composite Steel Floor Deck-Slabs. <http://www.sdi.org/wp-content/uploads/2017/02/ANSI-SDI-C-2017-Standard.pdf>.

2. ASTM (2018). Standard test methods for fire tests of building construction and materials, ASTM E119-18b, West Conshohocken, PA.
3. Bednar J., Wald F., Vodicka J. and Kohoutkova A. (2013). Experiments on membrane action of composite floors with steel fibre reinforced concrete slab exposed to fire. Fire Safety Journal, 59: 111-121.
4. Both K., Stark J.W.B. and Twilt L. (1992). Thermal shielding near intermediate support of continuous span composite slabs. Proceedings of 11th International Specialty Conference on Cold-formed Steel Structures, USA, 309-321.
5. Both C. (1998). The fire resistance of composite steel-concrete slabs. Ph.D. dissertation, Delft University of Technology, Delft, Netherlands.
6. European Committee for Standardization (CEN). (2005). Eurocode 4 Design of composite steel and concrete structures: Part 1.2: General rules, Structural fire design, EN 1994-1-2. CEN, Brussels.
7. Fedorov V.V. (1972). Theory of Optimal Experiments. Translated and edited by W.J. Studden and E.M. Klimko, Academic Press, New York.
8. Foster S., Chladná M., Hsieh C., Burgess I., Plank R. (2007). Thermal and structural behaviour of a full-scale composite building subject to a severe compartment fire. Fire Safety Journal, 42:183-199.
9. Guo S. (2012). Experimental and numerical study on restrained composite slab during heating and cooling. Journal of Constructional Steel Research, 69: 95-105.
10. Hamerlinck R., Twilt L. and Stark J. (1990). A numerical model for fire-exposed composite steel/concrete slabs. Proceedings of tenth International Specialty Conference on Cold-formed Steel Structures, USA, 115-130.
11. Hamerlinck, A. F. (1991). The behaviour of fire-exposed composite steel/concrete slabs. Ph.D. dissertation. Eindhoven University of Technology, Eindhoven, Netherlands.
12. Huang Z.H., Platten A. and Roberts J. (1996). Non-linear finite element model to predict temperature histories within reinforced concrete in fires. Building and Environment, 31(2): 109-118.
13. Huang Z.H., Burgess I.W. and Plank R.J. (2000). Effective stiffness modelling of composite concrete slabs in fire. Engineering Structures, 22(9): 1133-1144.
14. International Organization for Standardization (ISO). (2014). Fire-resistance tests – Elements of building construction, ISO 834, ISO, Geneva, Switzerland.
15. Jiang J., Main J.A., Sadek F. and Weigand J. (2017a). Numerical modeling and analysis of heat transfer in composite slabs with profiled steel decking. NIST Technical Note 1958, National Institute of Standards and Technology, Gaithersburg, MD.
16. Jiang J., Main J.A., Sadek F. and Weigand J. (2017b). Thermal performance of composite slabs with profiled steel decking exposed to fire effects. Fire Safety Journal. (in press)
17. Kolsek J., Saje M., Planinc I. and Hozjan T. (2014). A fully generalized approach to modelling fire response of steel-RC composite structures. International Journal of Non-Linear Mechanics, 67: 382-393.
18. Lamont S., Usmani A.S. and Drysdale D.D. (2001). Heat transfer analysis of the composite slab in the Cardington frame fire tests. Fire Safety Journal, 36: 815-839.
19. Lamont S., Usmani A.S. and Gillie M. (2004). Behaviour of a small composite steel frame structure in a "long-cool" and a "short-hot" fire. Fire Safety Journal, 39:327-357.
20. LSTC (2014). LS-DYNA Keyword User's Manual R7.1, Livermore Software Technology Corporation (LSTC), Livermore, California.
21. Li G.Q., Zhang N.S. and Jiang J. (2017). Experimental investigation on thermal and mechanical behaviour of composite floors exposed to fire. Fire Safety Journal, 89: 63-76.
22. Lim L.C.S., Buchanan A., Moss P. and Franssen J.M. (2004). Numerical modelling of two-way reinforced concrete slabs in fire. Engineering Structures, 26:1081-91.
23. Nag P.K. (2008). Heat and Mass Transfer. Tata McGraw-Hill Publishing, New Delhi.
24. Pantousa D. and Mistakidis E. (2013). Advanced modelling of composite slabs with thin-walled steel sheeting submitted to fire. Fire Technology, 49: 293-327.
25. Phan L., McAllister T.P., Gross J.L., and Hurley M.J. (2010). Best practice guidelines for structural fire resistance design of concrete and steel buildings. NIST Technical Note 1681, National Institute of Standards and Technology, Gaithersburg, MD.
26. Schwarz G. E. (1978). Estimating the dimension of a model, Annals of Statistics, 6(2): 461–464.

27. Shan Ba and V. Roshan Joseph (2015). MaxPro: Maximum Projection Designs. R package version 3.1-2. https://CRAN.R-project.org/package=MaxPro
28. R Core Team (2018). R: A language and environment for statistical computing. R Foundation for Statistical Computing, Vienna, Austria. URL https://www.R-project.org/.
29. Yu X.M., Huang Z., Burgess I.W. and Plank R.J. (2008). Nonlinear analysis of orthotropic composite slabs in fire. Engineering Structures, 30: 67-80.
30. Zhao B., Roosefid M., Breunese A. et al. (2011). Connections of steel and composite structures under natural fire conditions (COSSFIRE). Technical Report ECSC.

Appendix

In Tables A.1 and A.2 below, $l_{12} = (l_1 - l_2)/2$ (see slab dimensions in Figure 1); m.c. = moisture content; Num. = numerically computed fire resistance from finite-element analysis; NWC = normal-weight concrete, and LWC = lightweight concrete.

Table A.1. Summary of the 54 composite slab configurations used in the development of Eq. (3)

No.	Slab dimensions (mm)					m.c. (%)	Concrete type	Fire resistance (min)			Deviation from numerical (%)	
	h_1	h_2	l_2	l_{12}	l_3			Num.	EC4	Eq. (3)	EC4	Eq. (3)
1	50	40	30	10	40	10	NWC	74	45	85	−39	15
2	50	40	30	40	150	3	NWC	50	45	44	−10	−11
3	50	40	160	10	40	3	NWC	63	66	63	5	0
4	50	40	160	40	150	10	NWC	71	51	64	−28	−9
5	50	100	30	10	150	3	NWC	52	48	51	−8	−2
6	50	100	30	40	40	10	NWC	99	68	92	−31	−8
7	50	100	160	10	150	10	NWC	84	67	85	−20	1
8	50	100	160	40	40	3	NWC	79	105	84	33	6
9	125	40	30	10	150	3	NWC	147	159	149	8	1
10	125	40	30	40	40	10	NWC	249	166	244	−33	−2
11	125	40	160	10	150	10	NWC	252	168	251	−33	0
12	125	40	160	40	40	3	NWC	185	181	196	−2	6
13	125	100	30	10	40	10	NWC	255	170	261	−33	2
14	125	100	30	40	150	3	NWC	164	170	166	4	1
15	125	100	160	10	40	3	NWC	236	215	227	−9	−4
16	125	100	160	40	150	10	NWC	278	186	282	−33	2
17	50	40	30	10	150	10	LWC	68	37	77	−46	13
18	50	40	30	40	40	3	LWC	55	51	54	−7	−1
19	50	40	160	10	150	3	LWC	51	50	50	−2	−2
20	50	40	160	40	40	10	LWC	79	69	70	−13	−12
21	50	100	30	10	40	3	LWC	61	48	64	−21	5

22	50	100	30	40	150	10	LWC	73	50	67	−32	−9
23	50	100	160	10	40	10	LWC	113	104	120	−8	6
24	50	100	160	40	150	3	LWC	54	73	50	35	−8
25	125	40	30	10	40	3	LWC	186	205	184	10	−1
26	125	40	30	40	150	10	LWC	279	205	268	−27	−4
27	125	40	160	10	40	10	LWC	343	231	347	−33	1
28	125	40	160	40	150	3	LWC	206	214	205	4	−1
29	125	100	30	10	150	10	LWC	274	204	283	−26	3
30	125	100	30	40	40	3	LWC	220	232	219	5	0
31	125	100	160	10	150	3	LWC	231	231	230	0	−1
32	125	100	160	40	40	10	LWC	432	278	422	−36	−2
33	125	40	30	34	40	3	NWC	163	166	161	2	−1
34	50	100	30	17	40	3	NWC	63	57	64	−10	1
35	50	100	160	35	150	3	NWC	59	69	57	18	−3
36	125	40	160	17.5	40	10	NWC	280	182	278	−35	−1
37	50	100	30	13	150	10	NWC	79	48	79	−39	0
38	125	70	95	36.5	95	6.5	NWC	230	178	222	−22	−4
39	87.5	40	95	25	95	6.5	NWC	126	110	128	−13	2
40	87.5	70	30	28	95	6.5	NWC	124	109	128	−12	3
41	87.5	70	95	15	40	6.5	NWC	154	132	147	−14	−4
42	87.5	70	95	19	95	3	NWC	111	119	110	7	−1
43	87.5	70	95	25	95	6.5	NWC	138	119	138	−14	0
44	125	40	160	37	40	3	LWC	229	232	227	2	−1
45	125	40	30	27	150	3	LWC	181	204	183	13	1
46	125	40	30	16	40	10	LWC	285	208	289	−27	1
47	50	100	30	38	40	10	LWC	95	67	92	−29	−3
48	125	40	160	28	150	10	LWC	307	214	305	−30	−1
49	50	70	95	25	95	6.5	LWC	66	61	69	−8	4
50	87.5	40	95	24	95	6.5	LWC	144	132	138	−8	−4
51	87.5	70	160	36.5	95	6.5	LWC	154	152	162	−1	5
52	87.5	70	95	19.5	150	6.5	LWC	140	136	138	−3	−1
53	87.5	70	95	27.5	95	10	LWC	180	143	182	−21	1
54	87.5	70	95	26.5	95	6.5	LWC	155	143	150	−8	−3

Table A.2. Summary of the 32 composite slab configurations used for verification of Eq. (3)

No.	Slab dimensions (mm)					m.c. (%)	Concrete type	Fire resistance (min)			Deviation from numerical (%)	
	h_1	h_2	l_2	l_{12}	l_3			Num.	EC4	Eq. (3)	EC4	Eq. (3)
55	53.75	55	49.5	29.5	89.5	8.25	NWC	78	58	80	−26	3
56	61.25	91	101.5	23.5	144.5	4.05	NWC	76	79	73	4	−3
57	68.75	73	140.5	11.5	100.5	6.15	NWC	103	94	104	−9	1
58	76.25	85	114.5	35.5	56.5	8.95	NWC	146	119	147	−18	1
59	83.75	43	75.5	20.5	45.5	5.45	NWC	117	110	120	−6	2
60	91.25	67	36.5	17.5	122.5	9.65	NWC	147	113	158	−23	7
61	98.75	61	153.5	26.5	67.5	3.35	NWC	146	145	146	−1	0
62	106.25	79	62.5	38.5	111.5	4.75	NWC	159	146	154	−8	−3
63	113.75	97	88.5	14.5	78.5	7.55	NWC	221	165	217	−25	−2
64	121.25	49	127.5	32.5	133.5	6.85	NWC	208	165	207	−21	0
65	53.75	55	49.5	29.5	89.5	8.25	LWC	76	59	78	−22	2
66	61.25	91	101.5	23.5	144.5	4.05	LWC	73	85	74	16	1
67	68.75	73	140.5	11.5	100.5	6.15	LWC	104	105	106	1	2
68	76.25	85	114.5	35.5	56.5	8.95	LWC	158	139	163	−12	3
69	83.75	43	75.5	20.5	45.5	5.45	LWC	133	131	121	−2	−9
70	91.25	67	36.5	17.5	122.5	9.65	LWC	165	134	169	−19	2
71	98.75	61	153.5	26.5	67.5	3.35	LWC	174	178	160	2	−8
72	106.25	79	62.5	38.5	111.5	4.75	LWC	186	180	174	−3	−6
73	113.75	97	88.5	14.5	78.5	7.55	LWC	255	204	265	−20	4
74	121.25	49	127.5	32.5	133.5	6.85	LWC	252	209	248	−17	−2
75	85	75	120	32	120	5	LWC	129	140	131	9	1
76	85	75	120	32	120	7	LWC	142	140	148	−1	4
77	50	75	120	32	120	5	LWC	60	64	62	7	4
78	125	75	120	32	120	5	LWC	254	227	249	−11	−2
79	85	50	120	32	120	5	LWC	124	131	123	6	−1
80	85	100	120	32	120	5	LWC	133	146	138	10	4
81	85	75	80	32	120	5	LWC	127	134	125	6	−1
82	85	75	160	32	120	5	LWC	130	144	136	11	4
83	85	75	120	32	80	5	LWC	143	147	140	3	−2
84	85	75	120	32	160	5	LWC	122	137	121	12	−1
85	85	75	120	5	120	5	LWC	133	135	131	2	−2
86	85	75	120	65	120	5	LWC	125	143	131	14	4